AD NUMBER

AD878494

LIMITATION CHANGES

TO:

Approved for public release; distribution is unlimited.

FROM:

**Distribution authorized to U.S. Gov't. agencies and their contractors;
Administrative/Operational Use; DEC 1970. Other requests shall be referred to Air Force Weapons Lab., Kirtland AFB, OH 45433.**

AUTHORITY

AFWL ltr 30 Apr 1986

AD 878 494

AUTHORITY:
AFWL etc
30 APR 86

AFWL-TR
70-146

FOCUSING OF APERTURED GAUSSIAN BEAMS AT LONG RANGES

Dale A. Holmes
Capt USAF

TECHNICAL REPORT NO. AFWL-TR-70-146

December 1970

AIR FORCE WEAPONS LABORATORY
Air Force Systems Command
Kirtland Air Force Base
New Mexico

AFWL-TR-70-146

AIR FORCE WEAPONS LABORATORY
Air Force Systems Command
Kirtland Air Force Base
New Mexico

When U. S. Government drawings, specifications, or other data are used for any purpose other than a definitely related Government procurement operation, the Government thereby incurs no responsibility nor any obligation whatsoever, and the fact that the Government may have formulated, furnished, or in any way supplied the said drawings, specifications, or other data, is not to be regarded by implication or otherwise, as in any manner licensing the holder or any other person or corporation, or conveying any rights or permission to manufacture, use, or sell any patented invention that may in any way be related thereto.

This report is made available for study with the understanding that proprietary interests in and relating thereto will not be impaired. In case of apparent conflict or any other questions between the Government's rights and those of others, notify the Judge Advocate, Air Force Systems Command, Andrews Air Force Base, Washington, DC 20331.

DO NOT RETURN THIS COPY. RETAIN OR DESTROY.

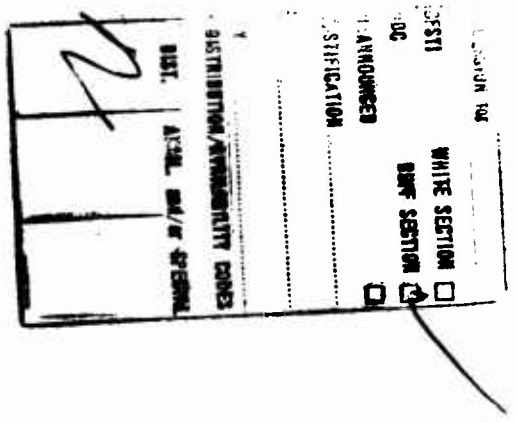

FOCUSING OF APERTURED GAUSSIAN BEAMS AT LONG RANGES

Dale A. Holmes
Capt USAF

TECHNICAL REPORT NO. AFWL-TR-70-146

FOREWORD

This research was peformed under Program Element 62301D, Project 0313, and was partially funded by the Advanced Research Projects Agency (ARPA).

Inclusive dates of research were 1 January 1970 through 15 September 1970. The report was submitted 12 October 1970 by the Air Force Weapons Laboratory Project Officer, Captain Dale A. Holmes (LRO).

This report has been reviewed and is approved.

Dale A. Holmes

DALE A. HOLMES
Captain, USAF
Project Officer

Edward N. Laughlin

EDWARD N. LAUGHLIN
Major, USAF
Chief, Optics Branch

C L Bamberson for CW

DONALD L. LAMBERSON
Colonel, USAF
Chief, Laser Division

ABSTRACT

(Distribution Limitation Statement No. 2)

Using Fresnel diffraction integrals, calculations have been made of the irradiance and power distributions in the vicinity of the focus for Gaussian beams focused through annular apertures. The effect of shifting the peak of the Gaussian aperture distribution from the aperture center was investigated and was found to be a small effect in some special cases. Gaussian and sinusoidal phase distortions of the aperture field were included in the calculations. It was found that these kinds of phase distortions generally reduce the focal plane irradiances in sometimes unpredictable ways. The numerical examples chosen for illustration should be useful in interpreting future experiments to be conducted by the Air Force Weapons Laboratory at the Sandia Optical Range.

CONTENTS

ILLUSTRATIONS

ILLUSTRATIONS (cont'd)

SYMBOLS

$I(r,z)$	Irradiance
J_o	Zero order Bessel function
$P(r)$	Focal plane power passing through a circle of radius r
$P(r,z)$	Power passing through a circle of radius r a distance z from the aperture
P_o	Power transmitted by aperture
R	Radius of curvature of aperture field phase front
R'	Correction to aperture field phase curvature because of a phase aberration
R''	Resultant aperture field phase curvature
T	Period of sinusoidal phase distortion
a	Inside radius of annular aperture
b	Outside radius of annular aperture
m	Amplitude of sinusoidal phase distortion
r,θ,z	Cylindrical coordinates
$u(r,z)$	Complex amplitude of diffracted field
$v(r)$	Complex amplitude of aperture field
v_o	Amplitude factor for aperture wave
w	Spot size of Gaussian aperture field
Δ	Amplitude of Gaussian phase distortion
Φ	Phase distortion of aperture field
λ	Vacuum wavelength
ω	Angular frequency
ρ,ϕ	Integration variables

SECTION I

INTRODUCTION

In this report, we consider some of the features of focusing 10.6 micron laser beams at kilometer ranges. To use a simple analytical approach we assume that the focusing device is an ideal on-axis Cassegrain telescope using spherical mirrors and that the field amplitude is Gaussian in magnitude over the final transmitting mirror of the telescope. Various simple kinds of phase distortion are introduced and the subsequent changes in the nature of the focused beam are discussed. Numerical illustrations have been prepared using specific parameter values rather than generalized dimensionless coordinates. The beam propagation is assumed to be diffraction limited; all other possible propagation factors, such as medium turbulence, are ignored in this work.

SECTION II

DIFFRACTION FORMULATION

To set up the problem, we define an (r, θ, z) cylindrical coordinate system. The final transmitting mirror of the telescope is assumed to lie in the z = 0 plane while the output beam travels in the positize z direction. We assume that the focusing problem can be handled by postulating a convergent Gaussian beam diffracted by an annular aperture in the z = 0 plane. The transmitting portion of the annular aperture occupies the region $a \leq r \leq b$. Physically, this can be interpreted as a collimated beam of radius a, entering the telescope and emerging as an annular focused beam of inside radius a and outside radius b, at the final mirror of the telescope. The diffraction calculations are applicable to the region z > 0 and are subject to the usual restrictions governing the use of Fresnel diffraction integrals in the scalar wave approximation. The case of the off-axis Cassegrain telescope can be considered by simply setting a = 0 in which case a is not interpreted as the radius of the input beam to the telescope.

The aperture field is taken as

$$v(r) = v_o \exp\left[-(r/w)^2 - i\pi r^2/\lambda R - i\Phi\right] \qquad (1)$$

In the sense of geometrical optics, the telescope is focused at a point on the z-axis a distance R from the z = 0 plane, hence, the plane z = R is called the focal plane. The focal range R is taken to be positive which implies a time variation given by exp[-iωt]. In (1), w is the beam spot size at the telescope transmitter mirror, λ is the vacuum wavelength, and Φ is a phase distortion which we shall restrict to be a function of r only. For most of the calculations described herein, the peak of the Gaussian distribution is on the z-axis as indicated by equation (1). In one later section, however, Equation (1) will be modified so that the peak of the Gaussian is shifted to the point (r, θ) = (Δx, o).

For convenience in later calculations, we shall assume that v_o is a real constant and is normallized so that total power P_o is always transmitted by the telescope. In the scalar wave approximation, we can then always determine v_o by the relation.

$$P_o = 2\pi \int_a^b dr\ r\ |v(r)|^2 \tag{2}$$

In all of the figures to follow, we take $P_o = 150$ watts. When $v(r)$ is given by equation (1) we have

$$v_o^2 = \left(2P_o/\pi w^2\right)/\left[\exp(-2(a/w)^2)-\exp(-2(b/w^2)\right] \tag{3}$$

Using the Fresnel diffraction integral, the scalar wave complex amplitude of the diffracted beam is

$$u(r,\ z) = (2\pi/\lambda z) \int_a^b d\rho\ \rho\ v(\rho)\ J_o(2\pi\rho r/\lambda z)\exp[i\pi\rho^2/\lambda z] \tag{4}$$

where we have omitted a phase factor on the right hand side of

$$-i\ \exp[i2\pi z/\lambda+i\pi r^2/\lambda z]$$

The irradiance of the diffracted beam is taken simply as $I(r,\ z) = |u(r,\ z)|^2$. In any plane z = constant, the power passing through a circle of radius r centered on the z-axis given by

$$P(r,\ z) = 2\pi \int_o^r d\rho\ \rho\ |u(\rho,\ z)|^2 \tag{5}$$

SECTION III

ON-AXIS IRRADIANCE

We now assume $\Phi = 0$ in equation (1) and $r = 0$ in equation (4). With these restrictions $I(0,z)$ can be written as

$$I(0,z) = v_o^2 \frac{NUM}{DEN} \tag{6}$$

where

$$NUM = \left[\exp(-(a/w)^2) - \exp(-b/w)^2)\right]^2$$

$$+ 4 \exp\left[-(a^2+b^2)/w^2\right] \sin^2 \left[\pi(b^2-a^2)(z-R)/2\lambda zR\right]$$

$$DEN = (\lambda z/\pi w^2)^2 + (z-R)^2/R^2$$

It is commonly assumed that $I(0,z)$ is symmetrical about the point $z = R$ but inspection of equation (6) reveals that this is not generally the case.

There is an optimization problem that one can readily solve using equation (6). We first consider that z is fixed at a constant value z_o and that R is variable. In this case $I(0,z_o)$ is regarded as a function of R and there exists an optimum value of R which maximizes $I(0,z_o)$. This optimum value is simply $R = z_o$. Physically, this means that an on-axis detector located at an arbitrary fixed location z_o will receive the largest signal when the telescope is focused such that $R = z_o$. This is true regardless of the values of a, b and w. If now the telescope focus is fixed at $R = z_o$ and the on-axis detector is physically moved along the z-axis toward the telescope, it is generally found that the detector signal will first increase, then pass through a maximum and then decrease.

Figures 1, 2, and 3 illustrate some of the predictions of equation (6). All three figures are calculated for a wavelength of 10.6 microns. In figures 2 and 3, the totally unobscured or complete Gaussian beam is shown as the solid line for comparison. The focal plane is located by the arrow on the abscissa. It is interesting to note that the focal plane irradiance for each case represented by

a broken line is approximately one-half of the focal plane irradiance for the free Gaussian. Both on-axis and off-axis Cassegrain telescopes were used to penetrate these curves. The figures verify that, for fixed a, b, P_o, and λ, the focal point irradiance is maximized for $\omega \to \infty$, i.e., the case of uniform illumination. An analytical proof of this maximization is as follows.

We evaluate the on-axis irradiance at the focal point, define $I_f = I(0,R)$, and obtain

$$I_f = \frac{2\pi w^2 P_o}{(\lambda R)^2} \cdot \frac{\exp\left[(b^2-a^2)/w^2\right]-1}{\exp\left[(b-a^2)/w^2\right]+1} \tag{7}$$

Taking the partial derivative of I_f with respect to w, we can obtain

$$\frac{\partial I_f}{\partial w} = \frac{4\pi w P_o}{(\lambda R)^2} \cdot \frac{\sum_{n=3}^{\infty} \left[(b^2-a^2)/w^2\right]^n \left[2^n-2n\right]/n!}{\left(\exp\left[(b^2-a^2)/w^2\right]+1\right)^2} \tag{8}$$

Now, since $2^n > 2n$ for $n \geq 3$, we see that $\partial I_f/\partial w$ is always positive and therefore I_f increases as w increases. The maximum value of I_f occurs in the limit $w \to \infty$ and is given simply by

$$\lim_{w \to \infty} I_f = \pi(b^2-a^2)P_o/(\lambda R)^2 \tag{9}$$

Note that we have restricted the above analysis to the case where the total beam power transmitted by the telescope is fixed at the constant value P_o.

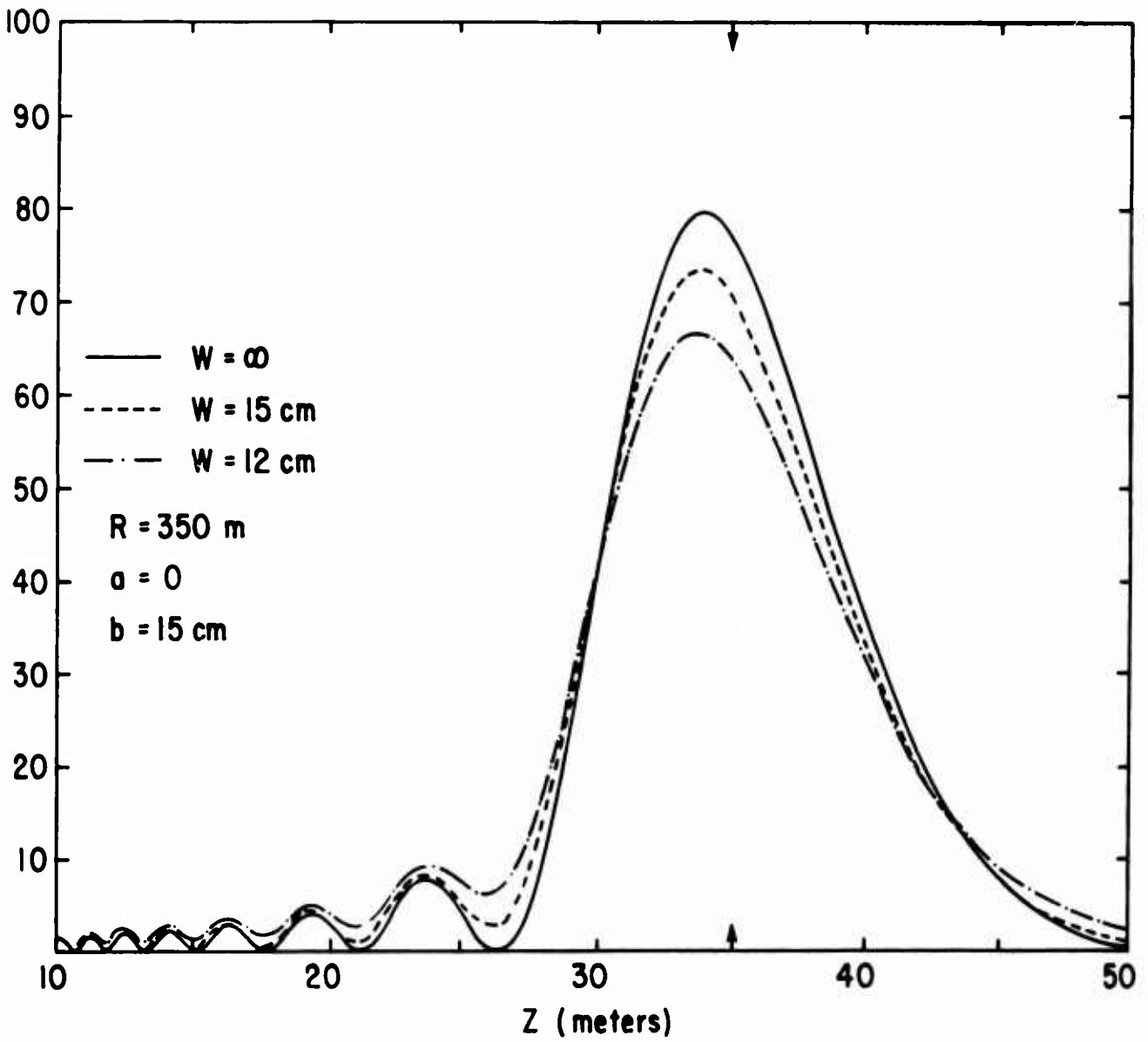

Figure 1. I(o,z) as a Function of z, Calculated from Equation (6)

(The ordinate has units of watts/cm^2 when P_o = 150 watts. The focal plane is located by the arrow on the abscissa.)

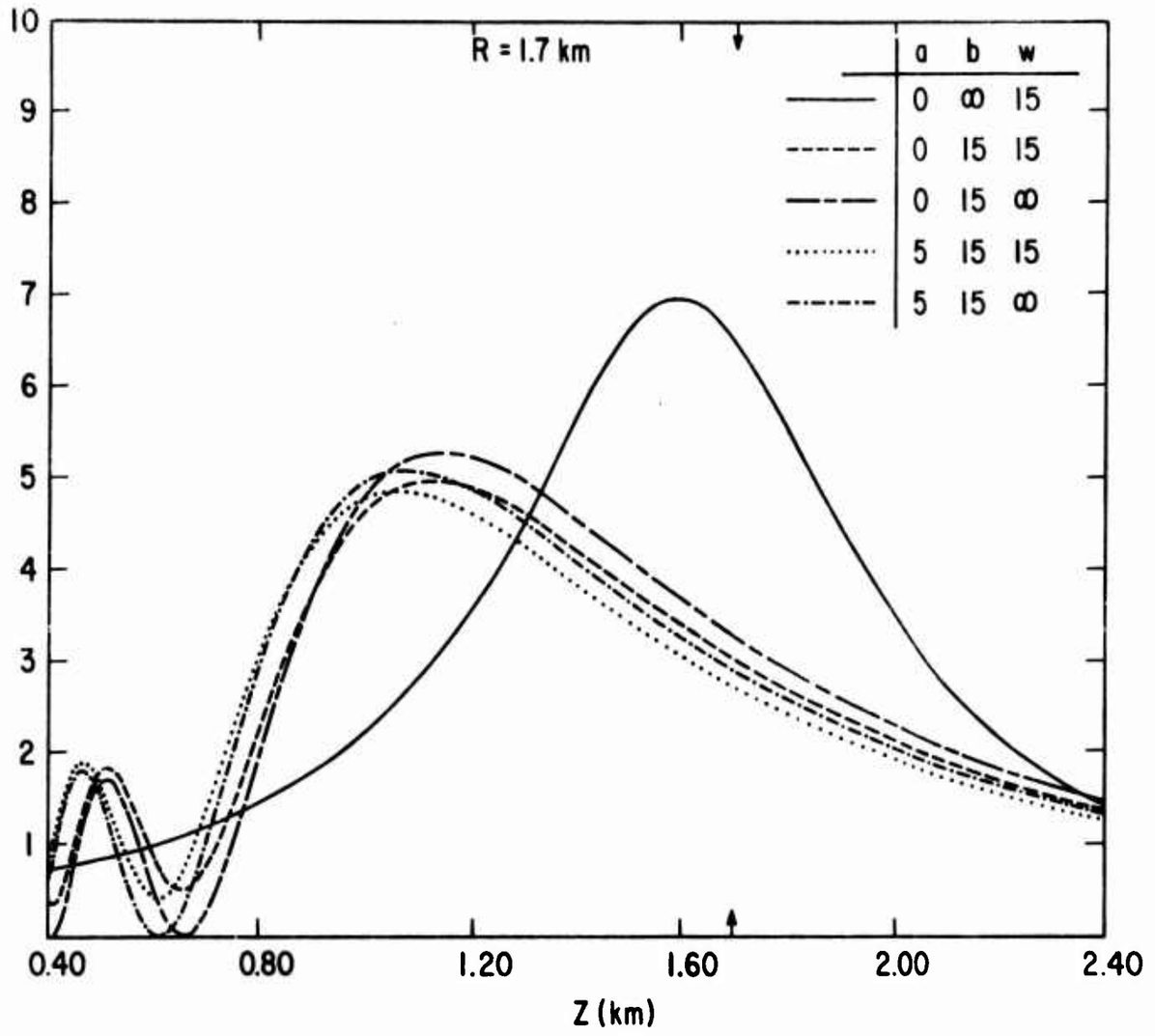

Figure 2. I(0,z) as a Function of z, Calculated from Equation (6)

(The ordinate has units of watts/cm^2 when the total beam power P_o = 150 watts. The wavelength is 10.6 microns.)

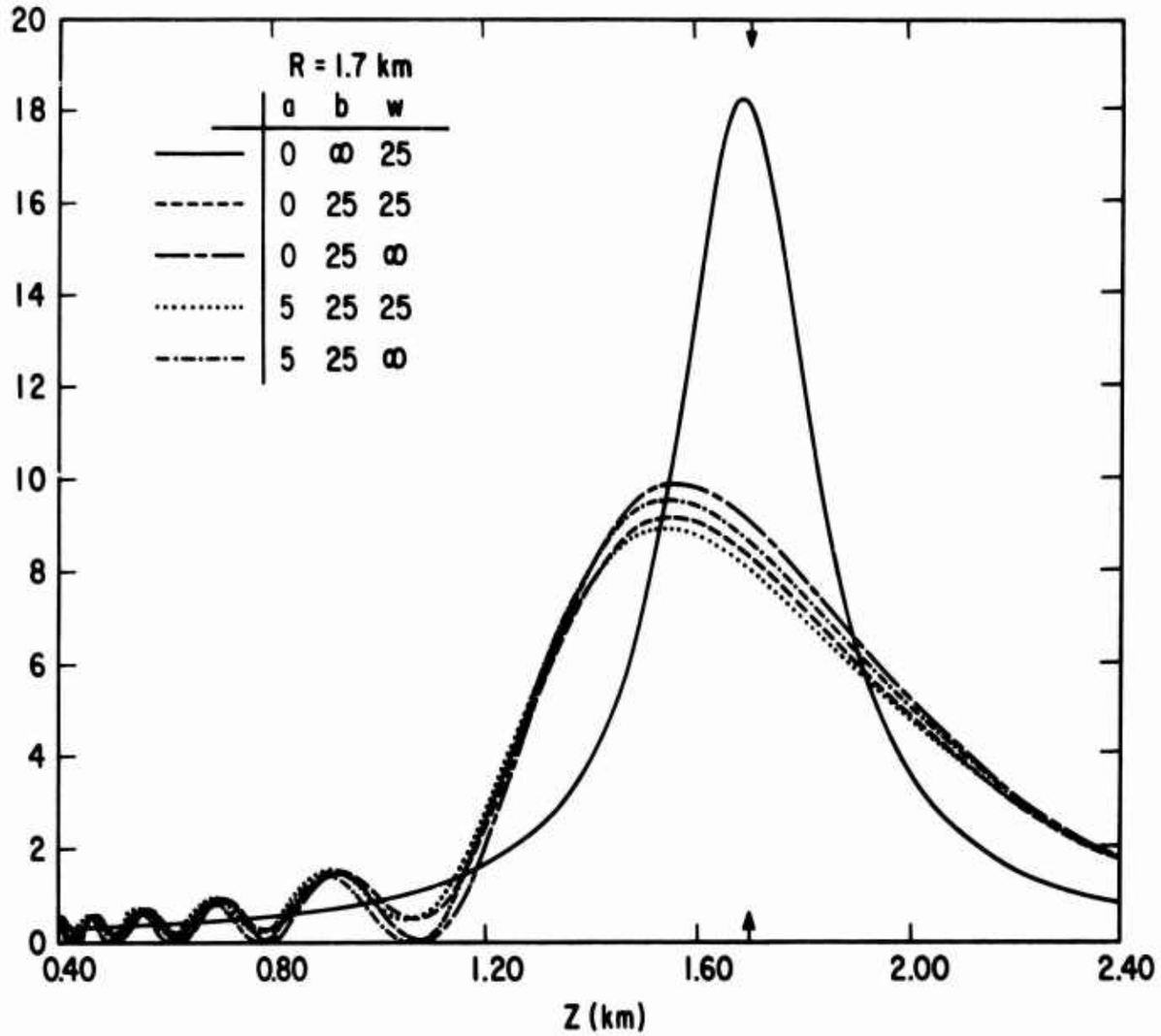

Figure 3. I(0,z) as a Function of z, Calculated from Equation (6)

SECTION IV

TRANSVERSE PROFILES

We shall now restrict our attention to the focal plane and examine the transverse irradiance and power profiles for ideal beams with $\Phi = 0$. Under these restrictions equation (4) reduces to

$$u(r,R) = (2\pi v_o/\lambda R)\int_a^b d\rho\ \rho\ J_o(2\pi r\rho/\lambda R)\exp\left[-(\rho/w)^2\right] \qquad (10)$$

There does not appear to be a simple way to evaluate equation (10) in terms of elementary tabulated functions, hence, numberical illustrations were prepared by computer integration of equation (10). Transverse irradiance profiles $I(r,R) = |u(r,R)|^2$ are shown in figures 4 and 5. The free Gaussian is again shown for comparison purposes. The curve for a=o and $w = \infty$ is the familiar Airy disk pattern whose first dark ring (zero) occurs for $r \simeq 0.61\ \lambda R/b$. The values chosen for a, b, w, λ, R and P_o are the same as for figures 2 and 3. The evaluation of v_o is given by equation (3).

The transverse power profiles (normalized to P_o) are given by

$$P(r)/P_o = (2\pi/P_o)\int_o^r d\rho\ \rho\ |u(\rho,R)|^2 \qquad (11)$$

and are shown in figures 6 and 7.

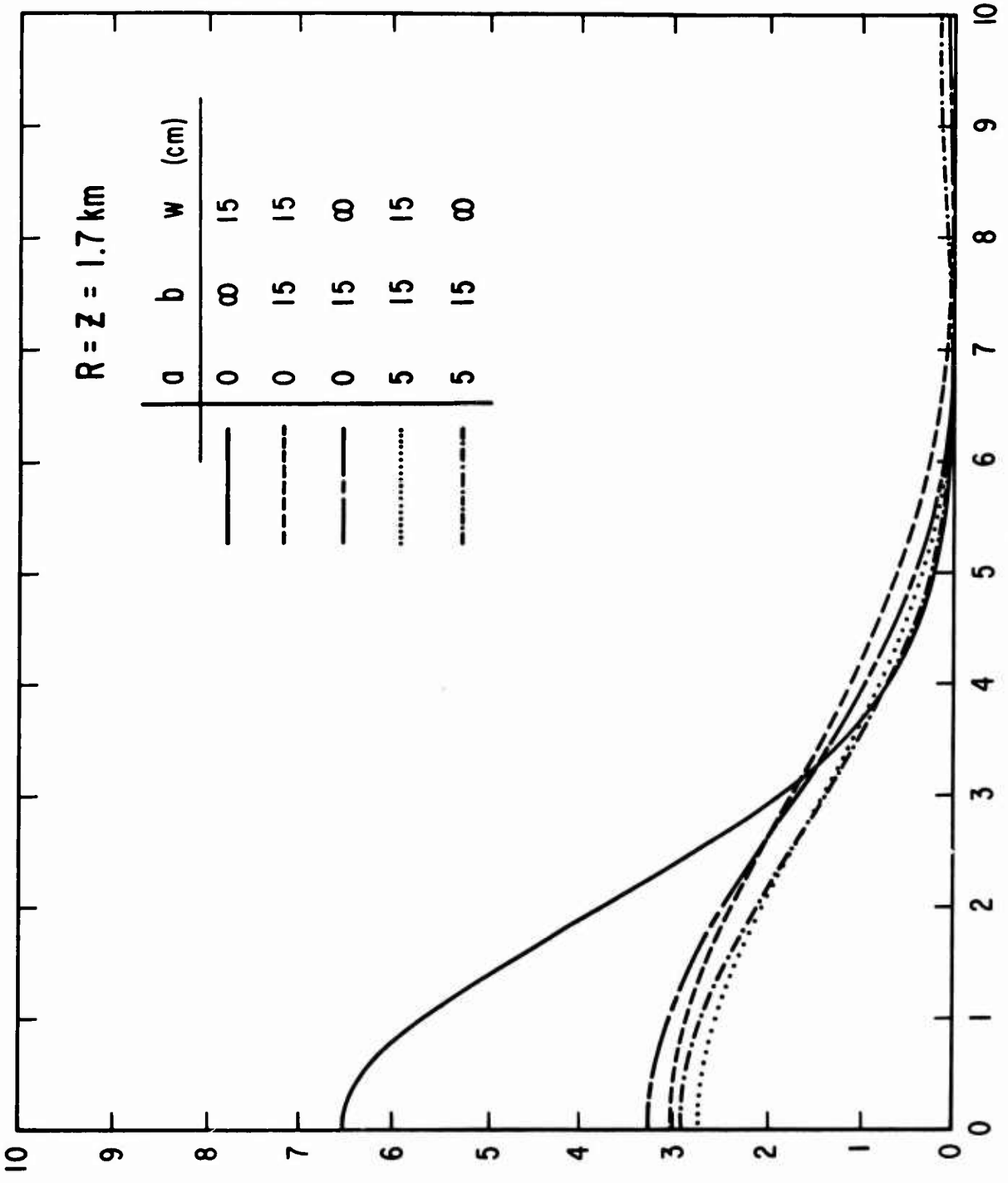

Figure 4. Transverse Irradiance Profile I(r,R) as a Function of r
(The ordinate has units of watts/cm^2 when the beam power P_o = 150 watts.)

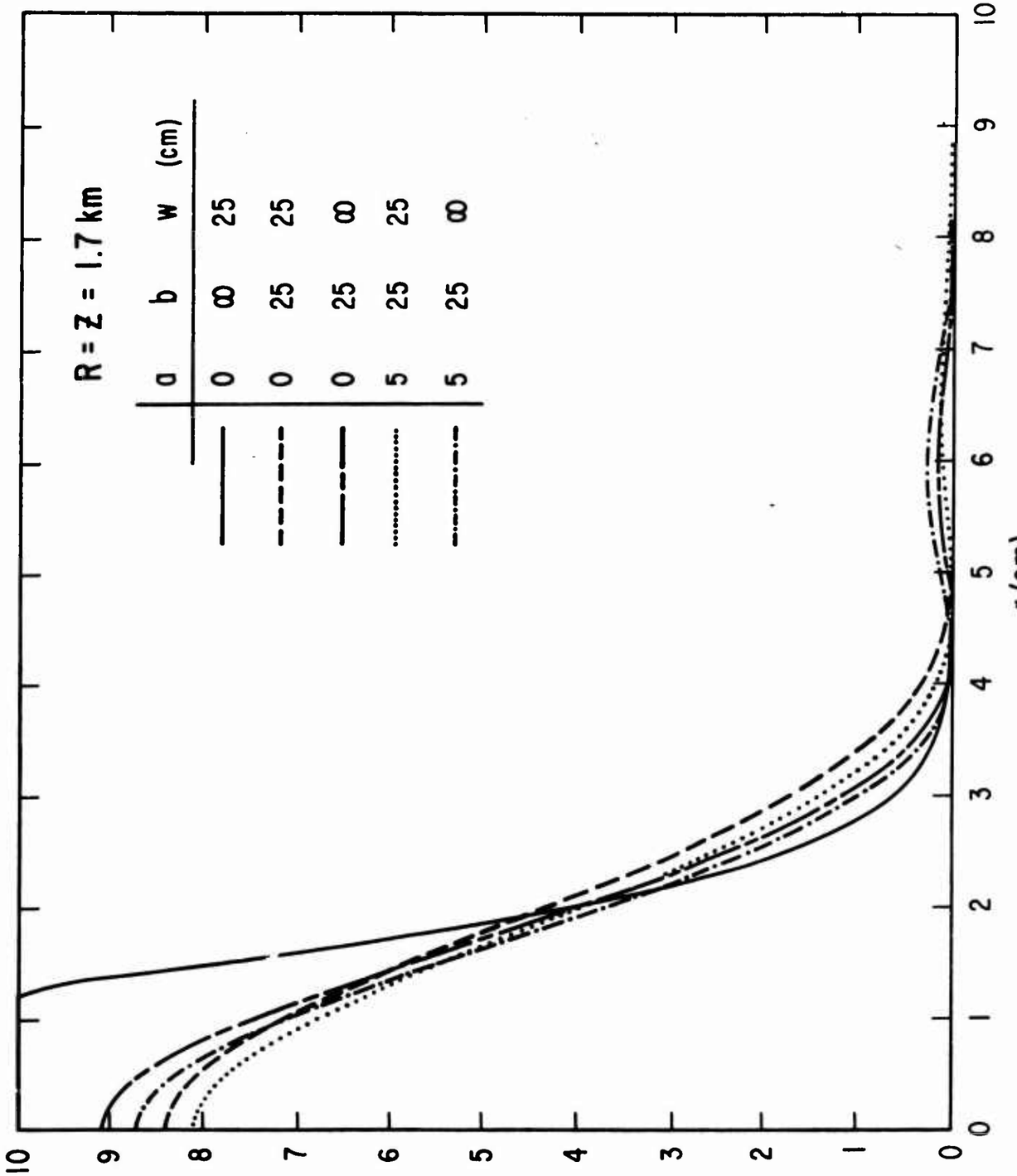

Figure 5. Transverse Irradiance Profile I(r,R) as a Function of r

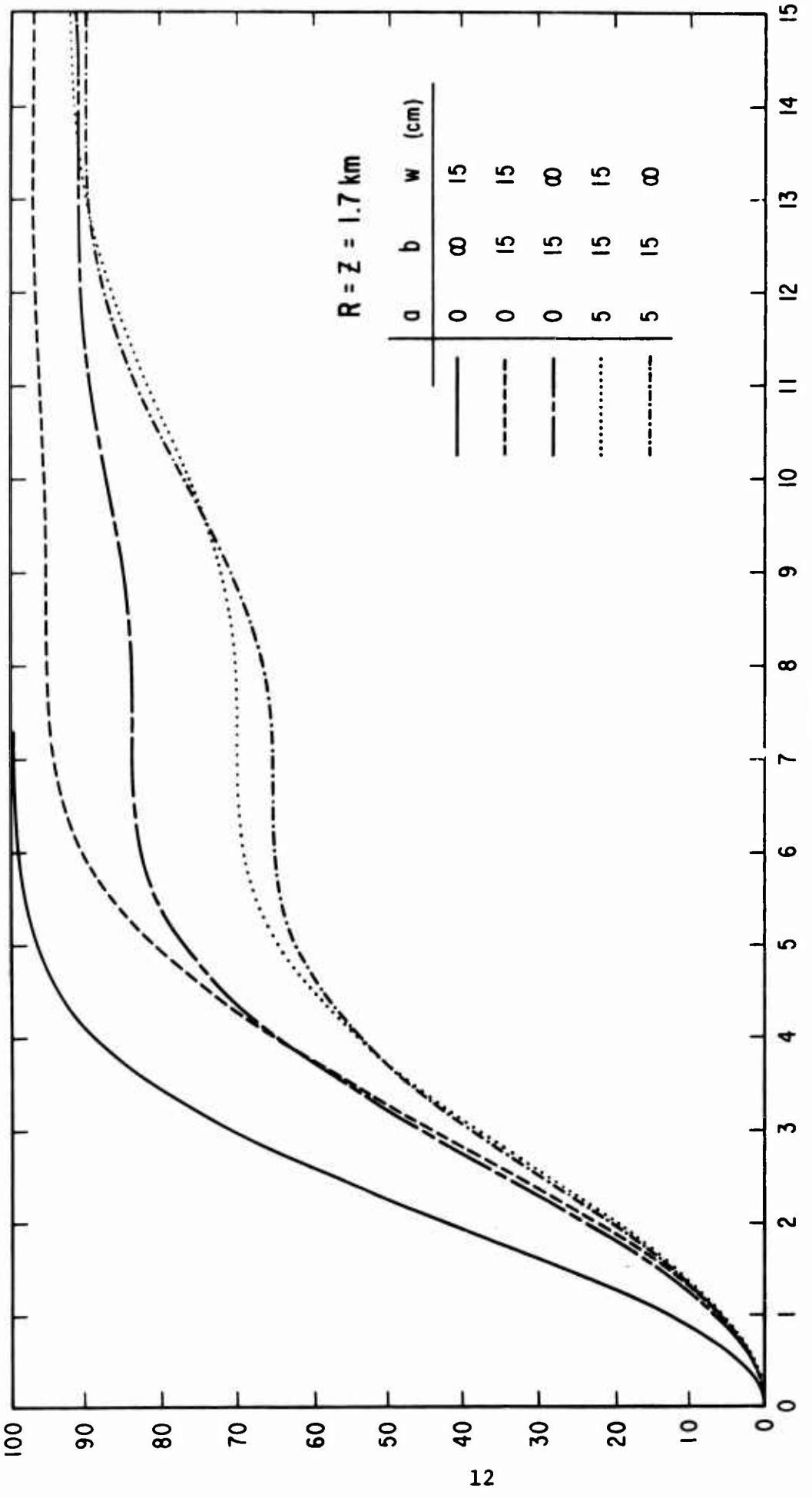

Figure 6. Normalized Focal Plane Power $P(r)/P_o$ (in percent) as a Function of Focal Plane Radius r
(The effects of the central obscuration in the on-axis Cassegrain telescope are most noticeable in the 60 to 90 percent range.)

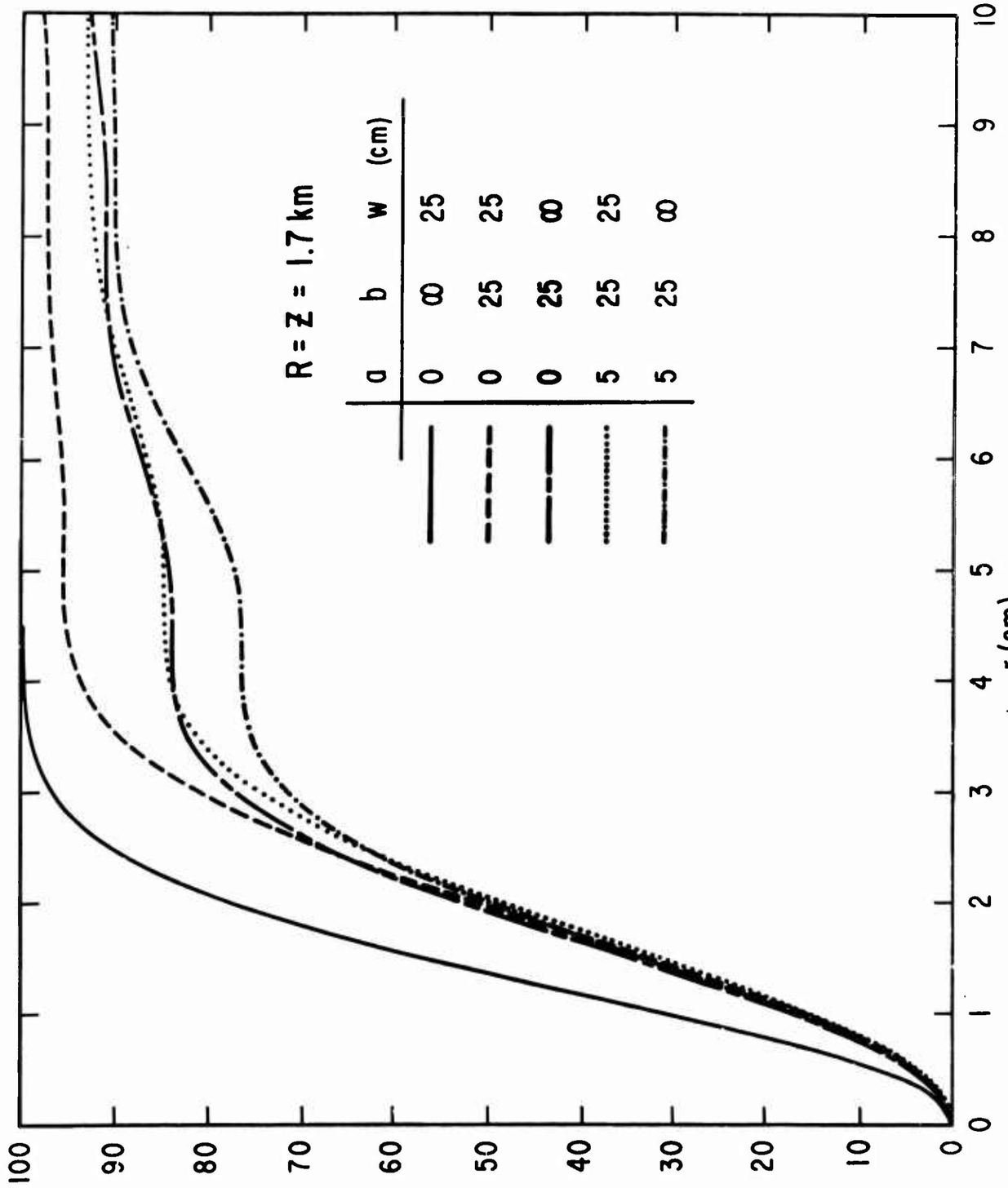

Figure 7. Normalized Focal Plane Power $P(r)/P_o$ (in percent) as a Function of Focal Plane Radius r (The effects of the central obscuration in the on-axis Cassegrain telescope are most noticeable in the 75 to 90 percent range.)

SECTION V

GAUSSIAN PHASE DISTORTION

In this section we consider the case when the phase distortion in equation (1) is given by

$$\Phi = (2\pi\Delta/\lambda)\exp\left[-2(r/w)^2\right] \tag{12}$$

The motivation for assuming Φ of the form equation (12) is to provide a simple, though perhaps crude, model of the effects owing to beam heating of mirror surfaces. Every mirror in the optical train prior to the telescope and even including the telescope mirrors absorbs a small fraction of the beam power. This small fraction is not insignificant, however, because the absorbed energy is converted to heat near the surface of the mirror and this heat forces dimensional changes in the mirror surface. The simplest possible model is to postulate that each mirror expands in a direction normal to its reflecting surface by an amount proportional to the local beam irradiance. Thus a normally plane mirror surface will become a convex Gaussian surface when subjected to a Gaussian local irradiance distribution.

By neglecting near field diffraction between mirrors, one then arrives at the Gaussian phase term as given in equation (12). Such a phase distortion can be visualized as consisting of two significant components: a quadratic term in r plus a more complex function. Thus we could write equation (12) as

$$\Phi = (2\pi\Delta/\lambda)-\left\{\pi r^2/\lambda R'\right\}+\left\{(2\pi\Delta/\lambda)\exp\left[-2(r/w)^2\right]-(2\pi\Delta/\lambda)+(\pi r^2/\lambda R')\right\} \tag{13}$$

where R' is not specified as yet. In equation (13), the first term in braces $\{\}$ can be interpreted as a distortion component that only changes the focal point (or, more properly, image point) of the telescopic system. If w is comparable to b, it is found numerically that there exists an R' such that the second term in braces in equation (13) has only a small effect on the diffraction calculations.

Since the Gaussian distortion model is only approximate and perhaps somewhat naive, no extensive effort has been expended to determine validated analytical solutions for R'. Possibly a simple least squares fit of $\Phi - 2\pi\Delta/\lambda$ to the paraboloid $-\pi r^2/\lambda R'$ would suffice. In this case, R' would then be given by

$$R' = (\pi/\lambda) \int dr\ r^5 \Big/ \int dr\ r^3 (2\pi\Delta/\lambda - \Phi) \tag{14}$$

The upper limit of the integrals in (14) would be b while some decision would have to be made whether to make the lower limit zero or a. The new focal point (or image point) would then be given by R'' where

$$1/R'' = 1/R - 1/R' \tag{15}$$

and R' is considered positive for positive Δ.

An alternative, and simpler, technique for determining R' is simply to expand Φ in an infinite series, yielding

$$\Phi = (2\pi\Delta/\lambda)\left[1 - 2(r/w)^2 + \text{higher order terms}\right] . \tag{16}$$

The quadratic term identifies R' as

$$R' = w^2/4\Delta \tag{17}$$

Equation (17) has the advantage of being simpler than equation (14) and for $w \geq b$ is probably adequate. The effective focal point is given simply by

$$1/R'' = 1/R - 4\Delta/w^2 \tag{18}$$

Calculations have been made of the on-axis irradiance assuming various numerical values for Δ/λ in equation (12). The diffraction integral was evaluated by using a series expansion for v(r) rather than direct computer integration. The diffracted field, evaluated on the z-axis, is given by

$$u(o,z) = (2\pi v_o/\lambda z)\sum_{n=o}^{\infty} \left[(-i2\pi\Delta/\lambda)^n \,/\, n!\right]$$

$$\cdot \int_a^b d\rho\ \rho\ \exp\left[\rho^2\left\{-(2n+1)w^2+i\pi(R-z)/\lambda Rz\right\}\right] \qquad (19)$$

After evaluating the integral, u(o,z) becomes

$$u(o,z) = (\pi v_o/\lambda z)\sum_{n=o}^{\infty} \left[(-i2\pi\Delta/\lambda)^n/n!\ c_n\right]\left[\exp(-a^2c_n)-\exp(-b^2c_n)\right] \qquad (20)$$

where

$$c_n = (2n+1)/w^2 - \pi i\ (R-z)/\lambda Rz \qquad (21)$$

Equations (3), (20), and (21) were used to prepare figures 8, 9 and 10.

In figure 8, we show the on-axis irradiance $I(o,z) = |u(o,z)|^2$ as a function of distance from the telescope with the telescope focus fixed at 1.7 km. As Δ/λ increases the irradiance at z = 1.7 km decreases. If a 10.6 micron beam is turned on at time t = o and Δ depends on time thereafter in a known way, these curves could possibly be useful for depicting the time evolution of the on-axis irradiance.

Figure 9 shows that a large fraction of the distortion (Eq. (12)) contributes to an effective change in focus of the telescopic system and indicates that equation (17) is a reasonable approximation for $w \geq b$. The same conclusion is drawn from figure 10, which is an alternative description of the predictions of equation (20).

For each value of Δ/λ in figure 10, the telescope focus R was adjusted to locate the peak of the on-axis distribution at the axial point z = 1.7 km, which, it should be noted, is not the same as maximizing the irradiance at the location z = 1.7 km.

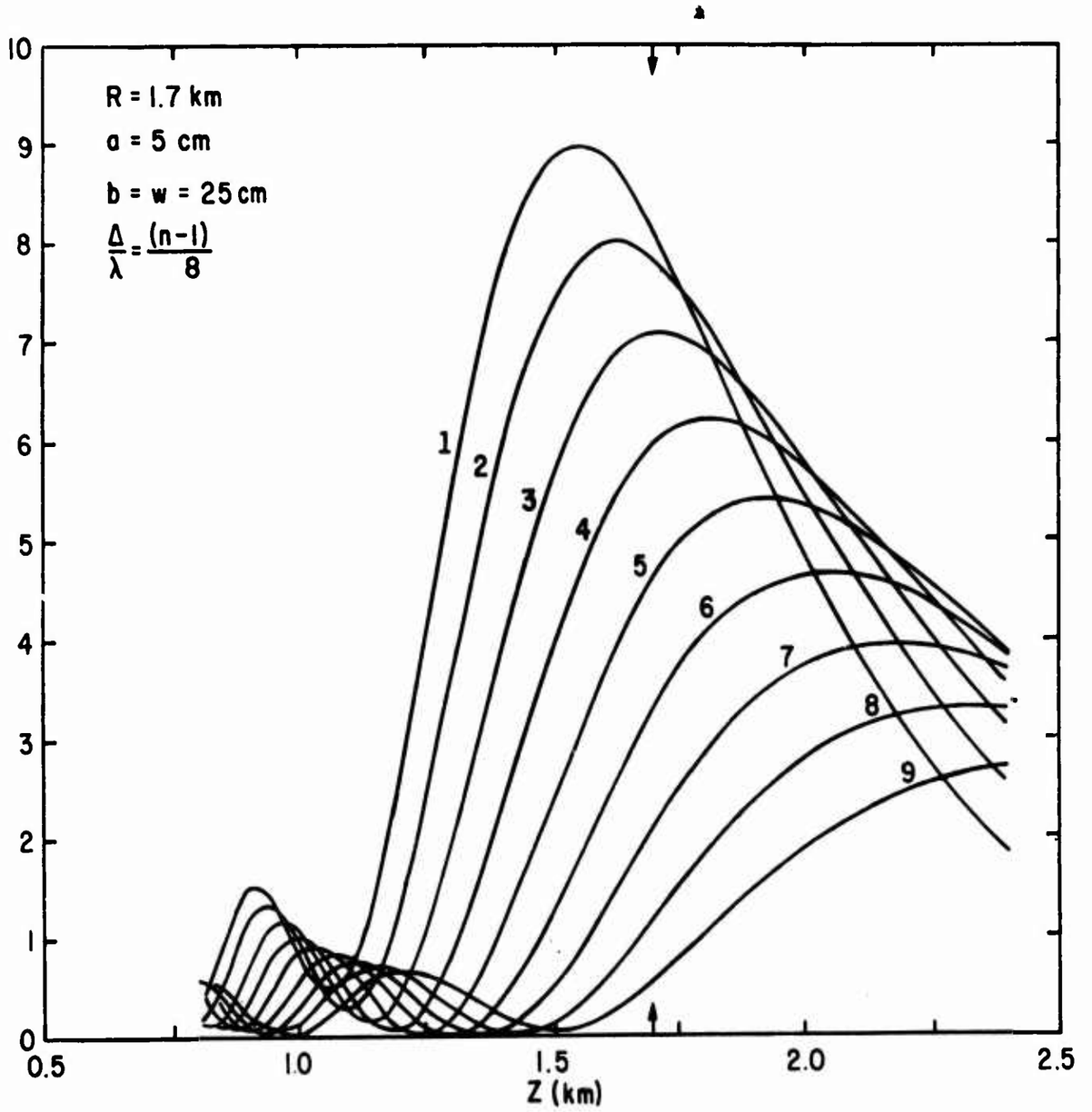

Figure 8. On-Axis Irradiance $I(0,z) = |u(0,z)|^2$ as a Function of z, Calculated from Equation (20)

(The integer n labels each curve and also specifies the value of Δ/λ associated with that curve.)

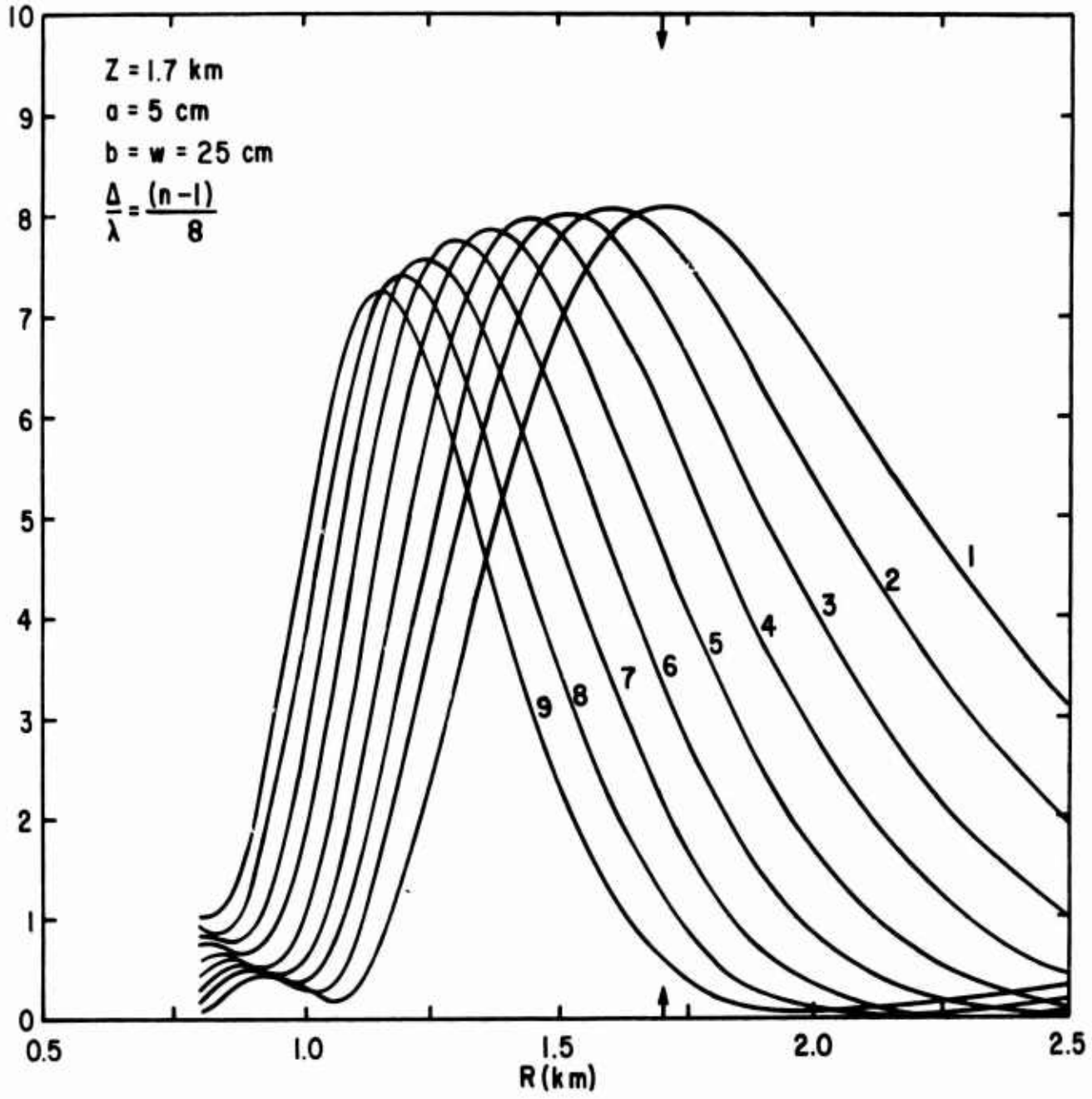

Figure 9. On-Axis Irradiance at a Fixed Distance z = 1.7 km as a Function of Telescope Setting R for Various Values of Δ/λ

(The integer n = 1, 2, ..., 9 which identifies each curve specifies the value of $\Delta/\lambda = (n-1)/8$.)

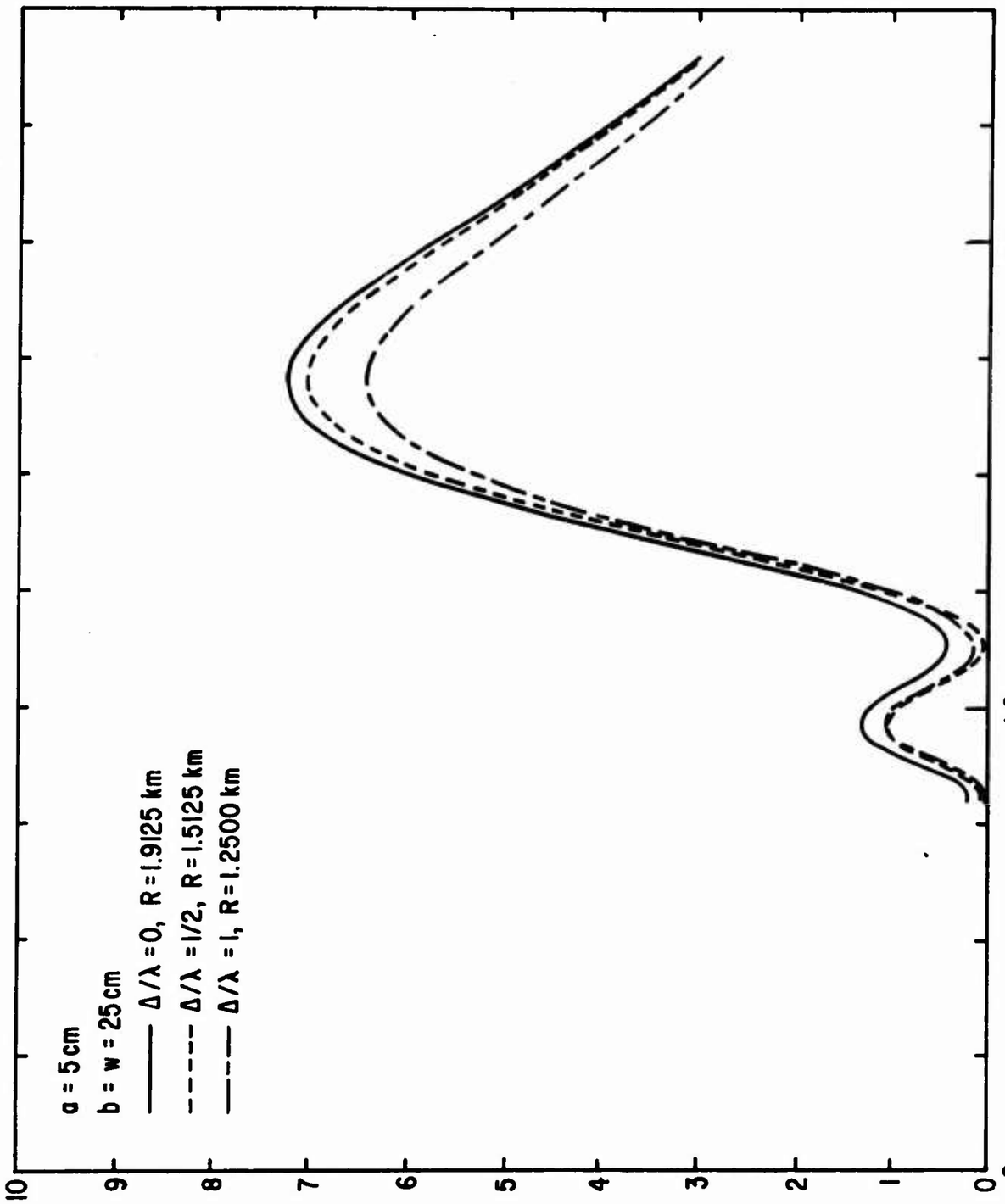

Figure 10. On-Axis Irradiance as a Function of Distance from the Telescope

SECTION VI

SINUSOIDAL PHASE DISTORTION

In this section, we consider the case when Φ is given by

$$\Phi = (2\pi m/\lambda)\cos(2\pi r/T) \tag{22}$$

where m specifies the peak value and T specifies the period of the sinusoidal phase distortion. One of the reasons for choosing to examine equation (22) is that the quadratic (change of focus) component should be small for $T < b$, which allows one to then directly investigate the degrading effects of the sinusoidal phase distortion on the focal plane irradiance and power distributions. In an approximate way, equation (22) does have connection with physical reality. For example, there exist mirrors that have surface deformation that depend on radius in a nearly periodic manner while possessing azimuthal symmetry.

When $T >> b$, we can see immediately that equation (22) represents mainly a change of focus with R' found from an expansion of equation (22):

$$-\pi r^2/\lambda R' = -(2\pi m/\lambda)(1/2)(2\pi r/T)^2$$

to yield

$$R' = T^2/4\pi^2 m \tag{23}$$

In this section, however, we are mainly interested in the case $T < b$. For this case we shall assume that the beam induced change of focus is negligible so that we can go directly to the telescope focal plane $R = z$ to investigate the transverse distributions.

To portray some of the effects of the cosinusoidal phase distortion (Eq. (22)) we proceed directly with numerical illustrations. In figure 11 we show the irradiance at the focal point as a function of peak distortion. It was found that the focal point irradiance was independent of T for the range 1 cm $\leq$ T $\leq$ 15 cm. Note that the focal point irradiance is nearly zero for $m/\lambda = 3/8$ and T = 1 cm. The entire transverse irradiance and power distributions are reduced in correspondence to the focal point irradiance for this case.

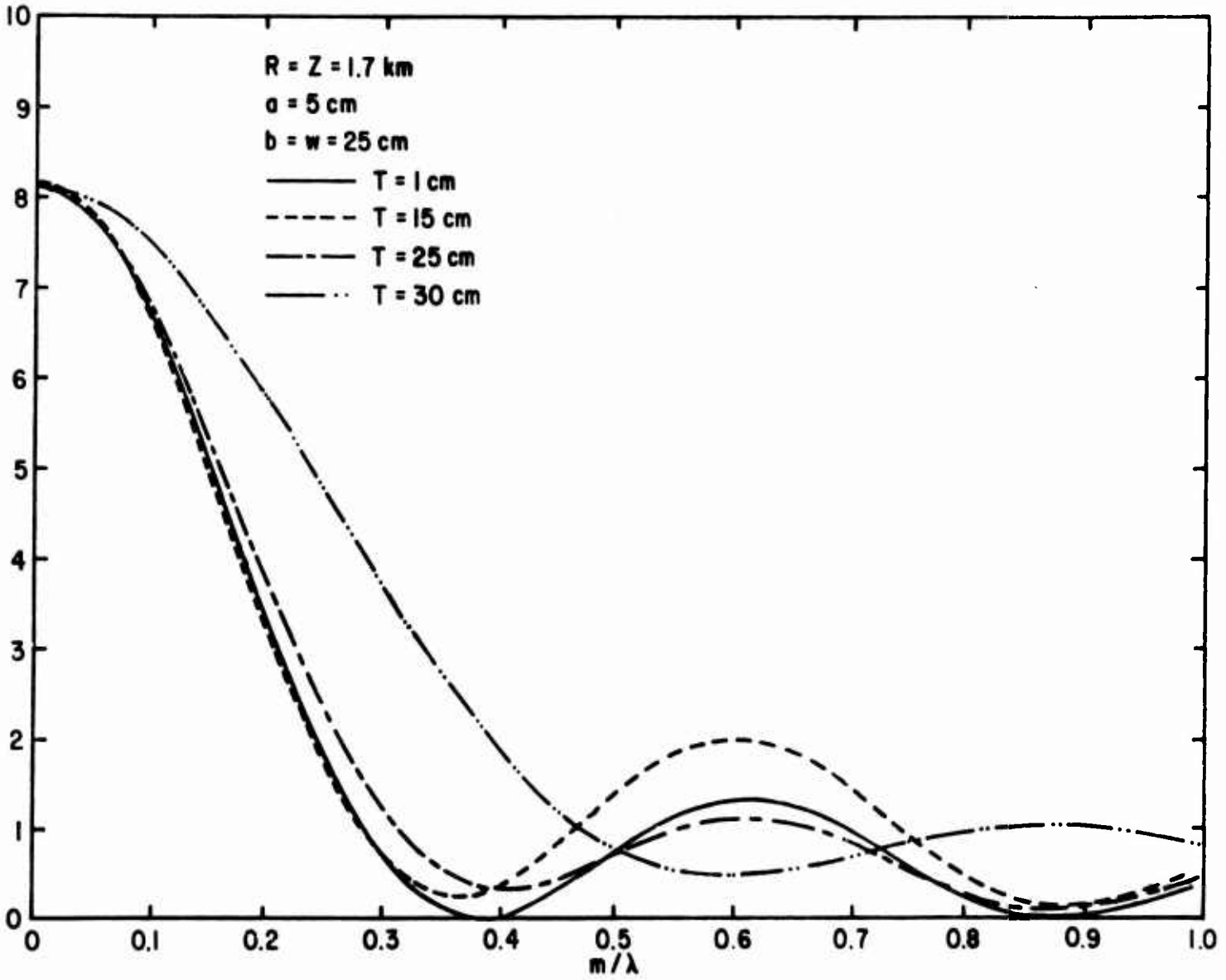

Figure 11. Focal Point Irradiance $I(0,R) = |u(0,R)|^2$ as a Function of Peak Distortion m/λ with Period T as the Parameter that Changes from Curve to Curve

Figure 12 shows the transverse irradiance and power distributions in the focal plane for a period T = 1 cm. Note that the numbers for the $m/\lambda = 3/8$ case are too small to show up on the scale of these graphs. The power distribution for the $m/\lambda = 3/8$ case is partially shown on an extended scale in figure 13. In figures 14 and 15, we show irradiance and power distributions for the somewhat larger spatial periods of T = 15 cm and T = 20 cm.

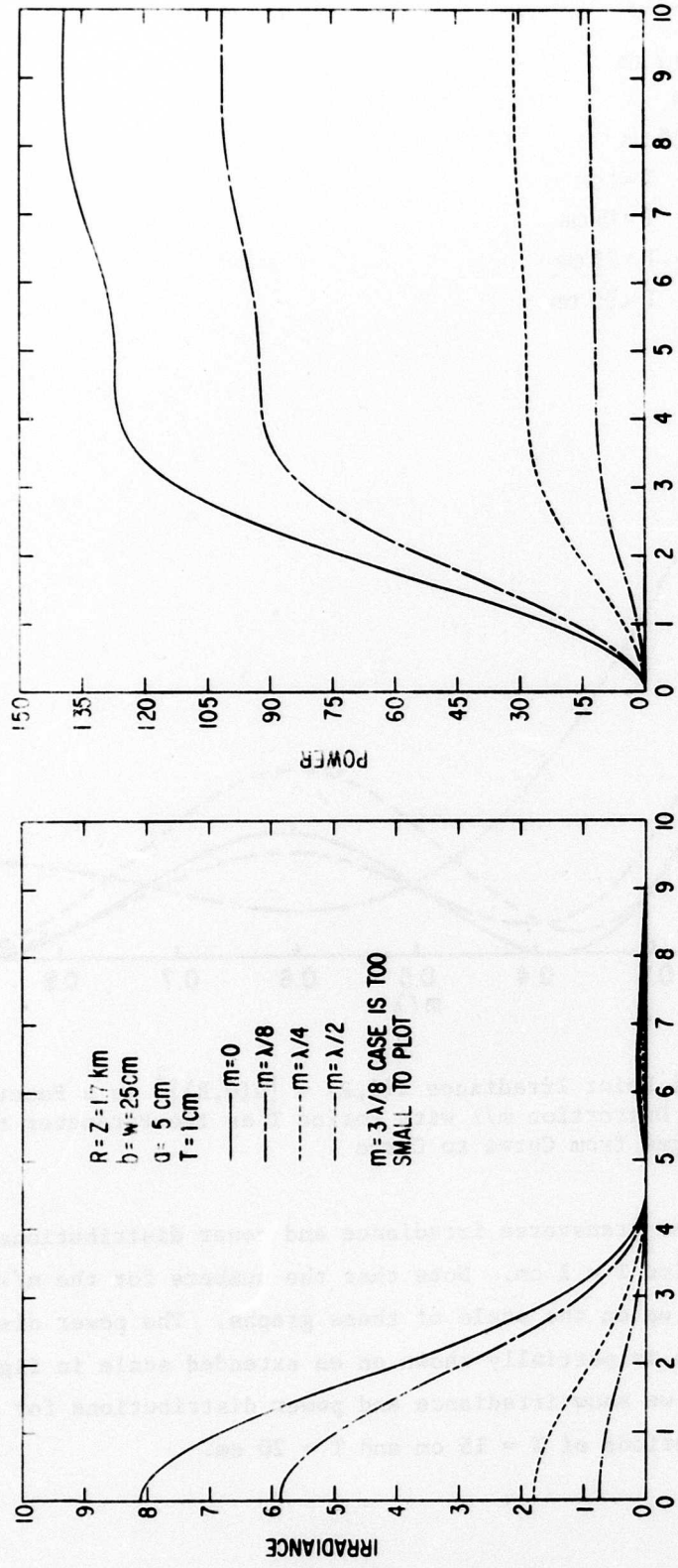

Figure 12. Focal Plane Irradiance and Power Profiles
(The period T = 1 cm for all curves.)

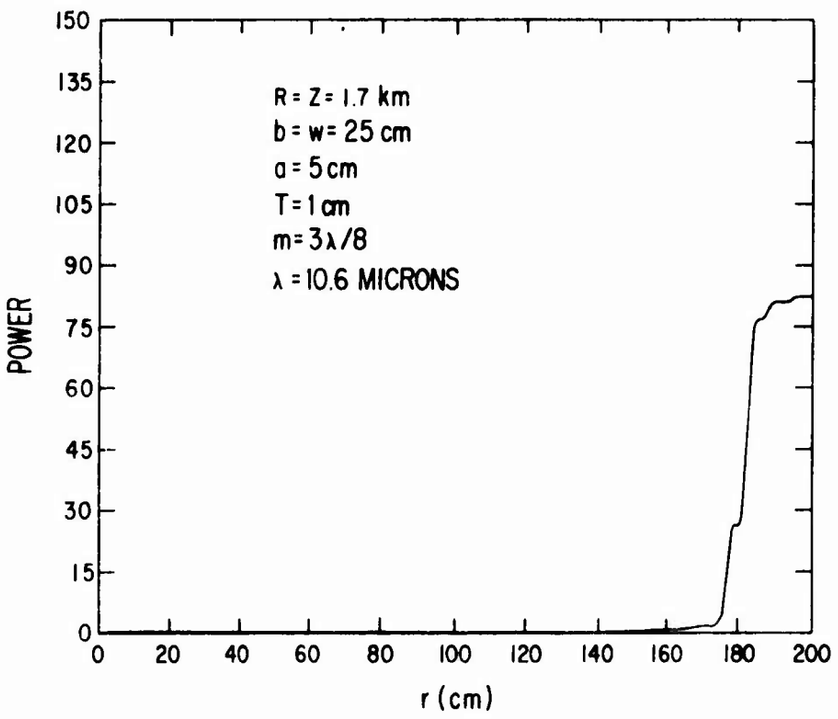

Figure 13. Part of the Focal Plane Power Distribution P(r,R) for m = 3λ/8 Case that did not show up in Figure 12

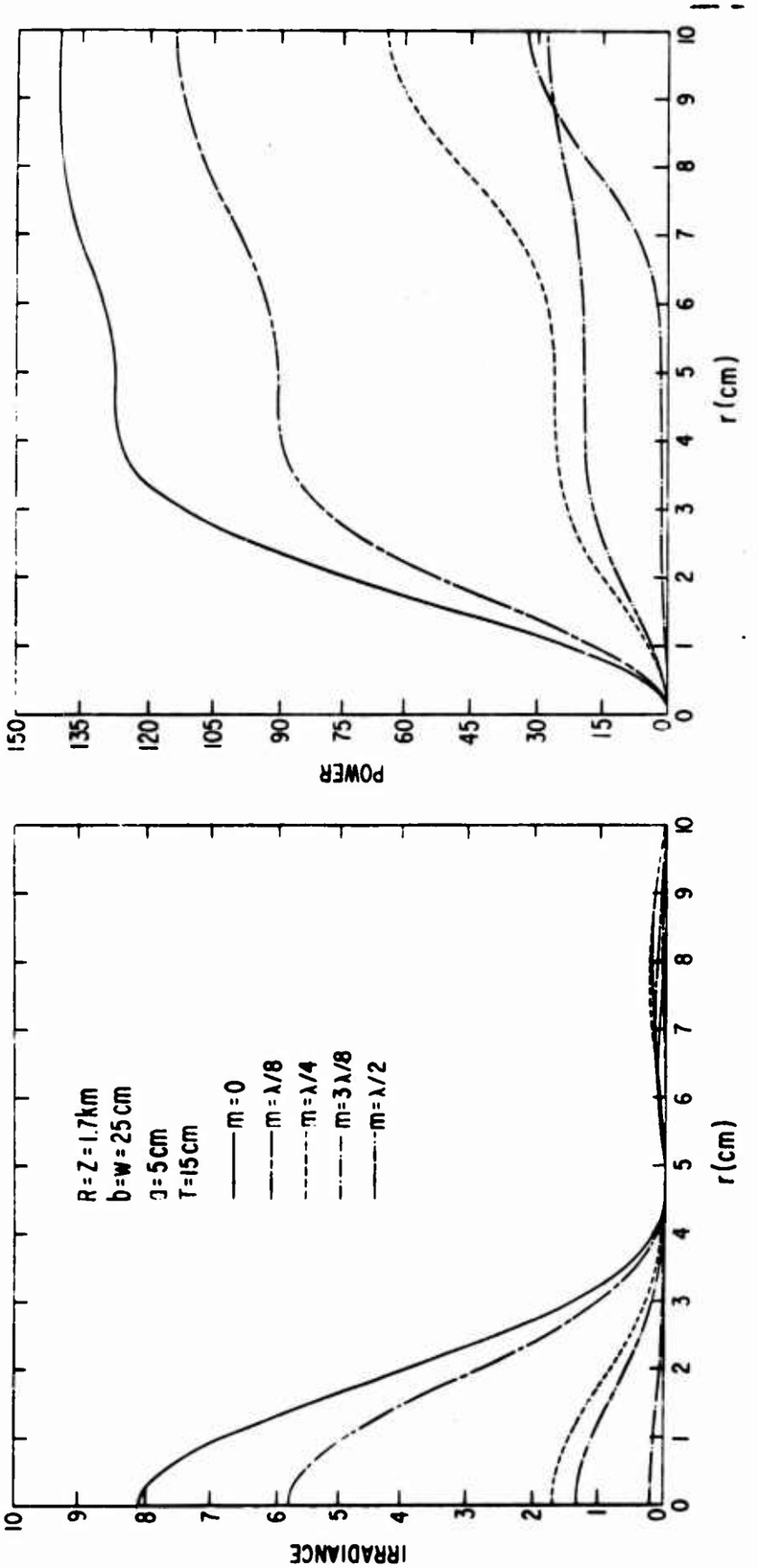

Figure 14. Focal Plane Irradiance and Power Profiles

(The period T = 15 cm for all curves.)

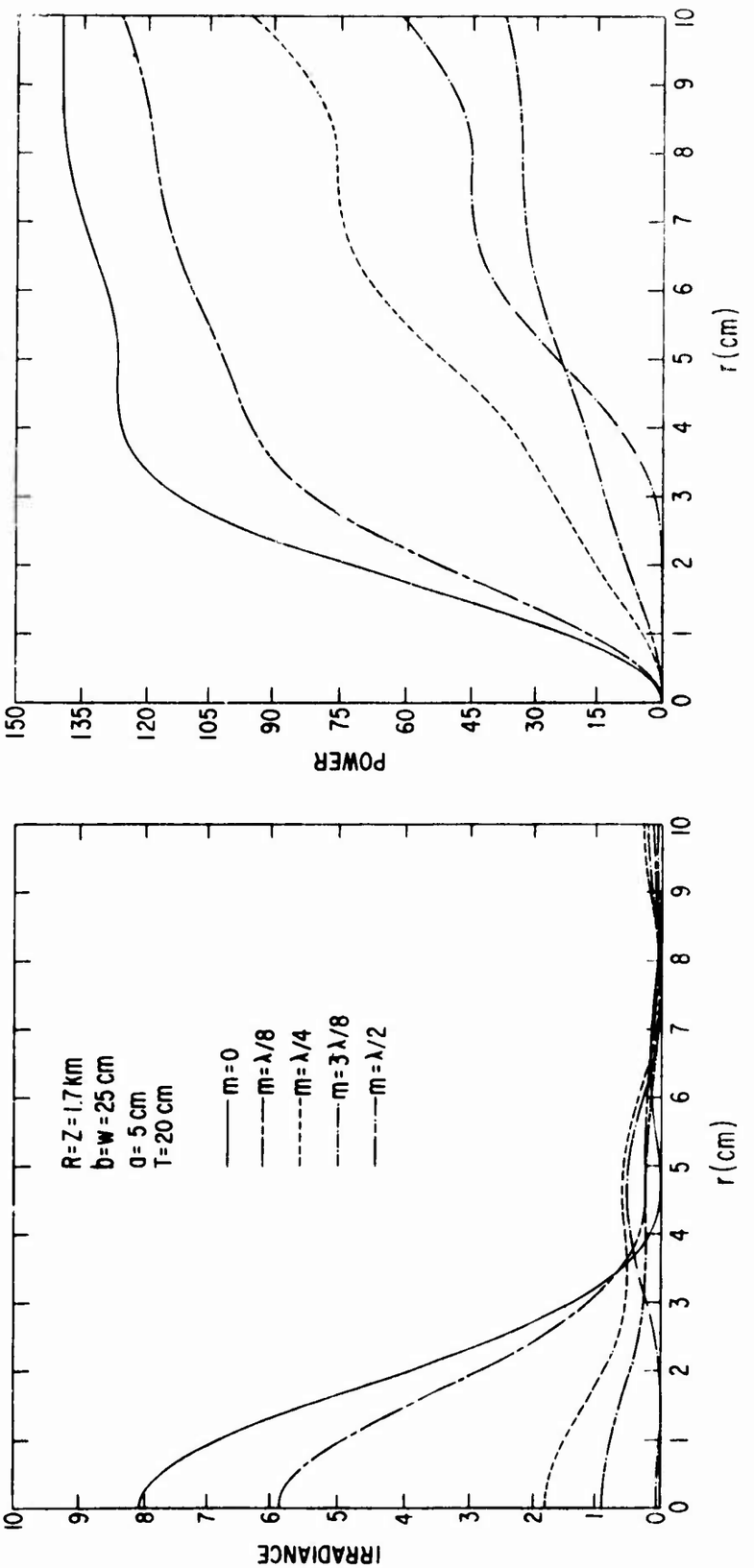

Figure 15. Focal Plane Irradiance and Power Profiles
(The period T = 20 cm for all curves.)

SECTION VII

DISPLACED GAUSSIAN PROFILES

In this section, we assume an ideal ($\phi = 0$) but displaced Gaussian aperture distribution. The aperture field is displaced by an amount Δx along the x-axis and, in cylindrical coordinates (r,θ), is given by

$$v(r,\theta) = v_o \exp\left[-\left\{(r\cos\theta-\Delta x)^2+(r\sin\theta)^2\right\}/w^2-i\pi r^2/\lambda R\right] \tag{24}$$

We still normalize v_o to a beam power P_o so that v_o is found from

$$P_o = \int_o^{2\pi} d\phi \int_a^b d\rho\ \rho\ |v(\rho,\phi)|^2 \tag{25}$$

The diffracted wave amplitude is defined as $u(r,\theta,z)$. We shall confine our attention to the focal plane $z = R$ so that $u(r,\theta,R)$ can be calculated by a Fraunhofer integral, as follows

$$u(r,\theta,R) = (\lambda R)^{-1} \int_o^{2\pi} d\phi \int_a^b d\rho\ \rho\ |v(\rho,\phi)|\ \exp\left[-2\pi i r\rho\ \cos(\theta-\phi)/\lambda R\right] \tag{26}$$

where we have again ignored purely phase factors on the right hand side of equation (26).

Figure 16 shows the results of some computer integrations of equation (25) and equation (26). The irradiance profile is taken along the x-axis in the focal plane where the displacement Δx has the greatest effect.

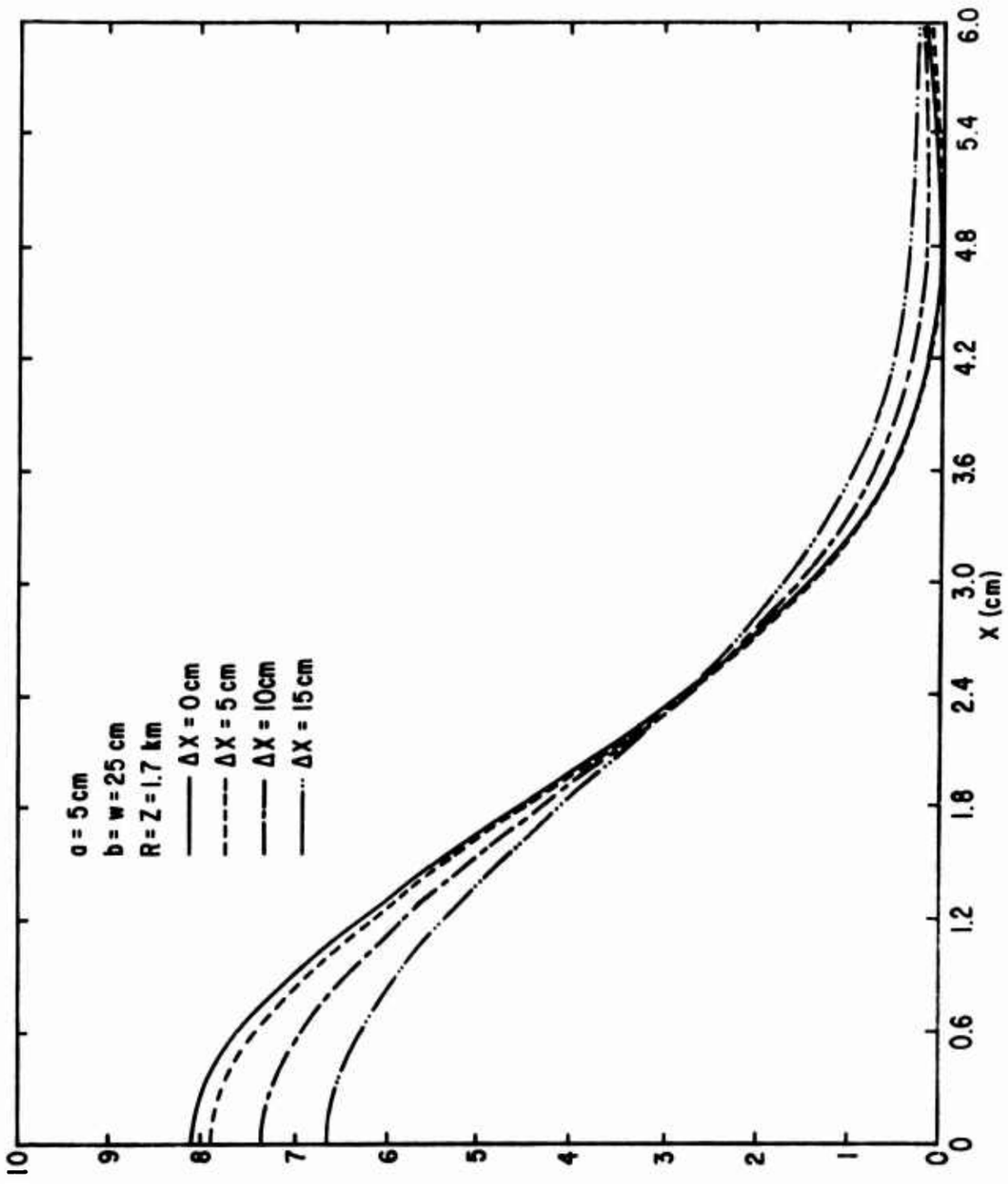

Figure 16. Focal Plane Irradiance Profiles $I(r,0,R) = |u(r,0,R)|^2$ along the X-Axis ($r = x$, $\theta = 0$) for Various Values of Aperture Field Displacement Δx

SECTION VIII

CONCLUSIONS AND SUMMARY

This report contains some specific calculations of Fresnel diffraction integrals using parameter values that should be useful in predicting the diffraction-limited propagation of Gaussian laser beams launched over long ranges. Both ideal and phase aberrated aperture distributions have been considered. It was found that Gaussian phase distortions of small value generally result in an effective change of focus in the telescopic system while cosinusoidal phase distortions of small period change the focal plane distributions in generally unpredictable ways.

The on-axis irradiance profiles show that, for long focal length infrared systems, these profiles are not symmetrical about the focal point. The possibilities for asymmetries of this nature have apparently been overlooked in advanced texts on optics. For example, in M. Born and E. Wolf, Principles of Optics, (1st edition, 1959), page 439, we find the statement that, "in the neighborhood of the focus the intensity distribution is symmetrical about the geometrical focal plane."

UNCLASSIFIED

Security Classification

DOCUMENT CONTROL DATA - R & D

(Security classification of title, body of abstract and indexing annotation must be entered when the overall report is classified)

1. ORIGINATING ACTIVITY (Corporate author)	2a. REPORT SECURITY CLASSIFICATION
Air Force Weapons Weapons Laboratory (LRO) Kirtland Air Force Base, New Mexico 87117	Unclassified
	2b. GROUP

3. REPORT TITLE

FOCUSING OF APERTURED GAUSSIAN BEAMS AT LONG RANGES

4. DESCRIPTIVE NOTES (Type of report and inclusive dates)

1 January 1970 through 15 September 1970

5. AUTHOR(S) (First name, middle initial, last name)

Dale A. Holmes, Captain, USAF

6. REPORT DATE	7a. TOTAL NO. OF PAGES	7b. NO. OF REFS
December 1970	36	

8a. CONTRACT OR GRANT NO.	9a. ORIGINATOR'S REPORT NUMBER(S)
b. PROJECT NO. 0313	AFWL-TR-70-146
c.	9b. OTHER REPORT NO(S) (Any other numbers that may be assigned this report)
d.	

10. DISTRIBUTION STATEMENT This document is subject to special export controls and each transmittal to foreign governments or foreign nationals may be made only with prior approval of AFWL (LRO), Kirtland AFB, NM 87117. Distribution is limited because of the technology discussed in the report.

11. SUPPLEMENTARY NOTES	12. SPONSORING MILITARY ACTIVITY
	AFWL (LRO) Kirtland AFB, NM 87117

13. ABSTRACT

(Distribution Limitation Statement No. 2)

Using Fresnel diffraction integrals, calculations have been made of the irradiance and power distributions in the vicinity of the focus for Gaussian beams focused through annular apertures. The effect of shifting the peak of the Gaussian aperture distribution from the aperture center was investigated and was found to be a small effect in some special cases. Gaussian and sinusoidal phase distortions of the aperture field were included in the calculations. It was found that these kinds of phase distortions generally reduce the focal plane irradiances in sometimes unpredictable ways. The numerical examples chosen for illustration should be useful in interpreting future experiments to be conducted by the Air Force Weapons Laboratory at the Sandia Optical Range.

DD FORM 1 NOV 68 1473

UNCLASSIFIED

Security Classification

14 KEY WORDS	LINK A		LINK B		LINK C	
	ROLE	WT	ROLE	WT	ROLE	WT
Focal plane irradiance						
Focal plane power						
Fresnel diffraction integral						
Phase aberrations						
Gaussian beams						
Cassegrain telescopes						
Aperture diffraction						